Prospects of transition interface sampling simulations for the theoretical study of zeolite synthesis†

Titus S. Van Erp,* Tom P. Caremans, Christine E. A. Kirschhock and Johan A. Martens

Received 16th October 2006, Accepted 20th December 2006
First published as an Advance Article on the web 25th January 2007
DOI: 10.1039/b614980d

The transition interface sampling (TIS) technique allows large free energy barriers to be overcome within reasonable simulation time, which is impossible for straightforward molecular dynamics. Still, the method does not impose an artificial driving force, but it surmounts the timescale problem by an importance sampling of true dynamical pathways. Recently, it was shown that the efficiency of TIS when calculating reaction rates is less sensitive to the choice of reaction coordinate than those of the standard free energy based techniques. This could be an important advantage in complex systems for which a good reaction coordinate is usually very difficult to find. We explain the principles of this method and discuss some of the promising applications related to zeolite formation.

I. Introduction

Gaining insight into zeolite formation has not only fundamental scientific importance, but could also accelerate momentous technological developments. The applications of zeolites are uncountable, ranging from cracking catalysis of crude oil, gas separation, detergent builders, and sensors for pharmaceutical formulations. The specific catalytic properties of zeolites lie in their unique open crystalline structure that incorporates cages or channels with typically nanoscale diameters. The growth of the open structure silicon dioxide polymorphs is mediated by so-called template molecules that can be removed out of the zeolite pores after the crystallization process. Besides template molecules, solvent, Si : Al ratio, temperature, pH, and many other factors play a role in determining which zeolite topology is formed. As each structure and composition has unique catalytic properties, the synthesis of new zeolite materials has been an important branch of chemical research. This development has progressed mainly on the basis of trial-and-error and 'chemical intuition' as a fundamental understanding of zeolite formation is lacking. The clear solution synthesis studies of silicalite-1 zeolites initiated by Schoeman *et al.*[1] were an important step forward for the experimental analysis. The use of clear solutions instead of gels made the analysis of zeolite synthesis much more accessible by experimental techniques. Since then, this model system has been the subject of many studies including X-ray and neutron scattering, infrared (IR) spectroscopy, nuclear magnetic resonance (NMR), and dynamic light scattering (DLS). These studies revealed that upon mixing tetraethylorthosilicate (TEOS), tetrapropylammonium hydroxide (TPAOH) and water at a certain ratio at room temperature sub-colloidal particles several nanometers in size are formed . Using the freeze drying technique,[2,3] these particles have been extracted from the solution and examined by various techniques such as solid state NMR, Fourier transform IR (FTIR), transmission electron microscopy (TEM), and atomic force microscopy (AFM). Various models for the structure of these particles have been proposed, ranging from amorphous bodies[4,5] to precise framework fragments.[6]

The formation of crystalline zeolite particles is initiated when this suspension is heated up to temperatures of 350 K. Light scattering experiments show that the intensity scattered by the suspension increases only slowly with time during the first period of the synthesis. This is then followed by a sharp increase, indicating the starting point of growth of what will become the final crystals. The first period can be associated with a nucleation process, in which a particle has to be formed with a size beyond its critical nucleation radius. The formation of zeolites thus consists of several stages: first a polymerization process which eventually leads to the formation of sub-colloidal particles, second the nucleation process, and finally crystal growth.

One of the difficulties in the investigation of the zeolite formation process is that the relevant length scales of the zeolite formation lie just in between the accessible length scale of NMR and diffraction techniques.[7] Moreover, it is unclear if freeze-dried extractions are identical to the silicate particles existing in solution. Since many experiments do not allow unequivocal interpretation, it is not a surprise that several crystallization mechanisms have been proposed. These theories concentrate on the structure and shape of the colloidal particles, how these particles are formed and how these particles finally contribute in the formation of the zeolite crystal.

Centre for Surface Chemistry and Catalysis, K.U. Leuven, Kasteelpark Arenberg 23, 3001 Leuven, Belgium. E-mail: Titus.VanErp@biw.kuleuven.be
† The HTML version of this article has been enhanced with colour images.

An example is the nanoslab hypothesis that was postulated by some of us. It was inspired by several experimental observations.[6,8,9] This theory assumes that at an initial stage precursor particles are formed which consist of 30 to 33 Si atoms enclosing a single template molecule. These precursors stick together in a block shaped particle, the nanoslab, that already has the correct crystalline structure. These particles finally form the zeolite by a 'clicking mechanism' when the solution is heated up. Others have claimed that the apparent evidence of the Si-30/33 precursor particle should be attributed to other Si containing species[10] or that the nanoshaped particle is actually an amorphous identity with a layer of template molecules around it.[4,5] The role of the nanosized particles in the nucleation and crystal growth has also been the subject of debate. According to some groups, the nanoparticles add one by one to the growing crystals.[11,12] Others regard the particles as monomer reservoirs: monomer dissolves into the solution and attaches to the growing nucleus.[13,14] Recent publications[14,15] state that an aggregative growth mechanism of discrete nanoparticles may dominate the early stage of the growth process. However, after a certain size is attained, the growth mechanism seems to switch to addition of low molecular species, probably monomers.

In conclusion, despite many years of abundant experimental research, zeolite synthesis still contains many mysteries. Therefore, this is a prototype example of a field of research where computer simulations could give invaluable information. However, truly realistic simulations of all stages in the zeolite synthesis are still a long way off, because the typical system sizes and timescales at which the zeolite formation takes place are generally beyond the capabilities of present computer resources. For the correct modeling of the nucleation process, the simulation box should at least be larger than the critical nucleus, a requirement that is out of limits for quantum mechanical calculations and demands the development of accurate reactive force fields.

So far fully quantum mechanical calculations using density functional theory (DFT) have been applied to silica polymerization clusters.[16,17] These studies showed the stronger stability of silicate 6 rings and linear polymers compared to smaller rings and branched polymers. pH effects were considered in ref. 18 and 19 by analyzing negatively charged silica clusters that are favorable to neutral ones in an alkaline environment. This study revealed that internal cyclization is preferred over further linear growth.[18] Barriers for oligomerization were significantly reduced for single charged clusters compared to neutral ones.[19]

Based on *ab initio* calculations or experimental data, several classical force fields have been developed.[20–24] These potentials allow the study of larger systems including solvent and template molecules. However, the existing potentials do not yet describe the breaking and making of chemical bonds very accurately, which presumably requires complex many-body terms and polarizable force fields. Still, studies using these approximate potentials can give valuable information. For instance, classical molecular dynamics (MD) simulations have shed some light on the role of solvent and template molecules.[25,26] These simulations showed that, contrary to fully formed cages and rings, open structures collapsed in the presence of solvent, unless it contained strongly bonded template molecules. The early stages of silica polymerization dynamics were studied by Rao and Gelb[27] at high temperatures $\gtrsim$1500 K. These elevated temperatures were required as up to 600 K, no polymerization reaction could be observed within the nanosecond simulation periods. They found that both the monomer incorporation and cluster–cluster aggregation were important mechanisms for diluted solutions, while the first mechanism was dominant in the concentrated systems. Using an implicit solvent model not including template molecules, Wu and Deem analyzed the free energy barriers and critical cluster sizes as a function of pH and Si-monomer concentration at ambient conditions using a series of advanced Monte Carlo (MC) techniques.[28] They found that the critical clusters for the polymerization contained relatively few ($\approx$30–40) Si atoms. No attempt was made to derive reaction rates by calculating transmission coefficients. Even larger systems and timescales have been simulated using lattice models[29,30] and kinetic MC (KMC).[31] Relative rates for different crystal growth mechanisms *via* kink and edge sites can be derived by mimicking atomic force micrographs *via* atomistic simulations.[32–34] Still, even KMC simulations are usually restricted to growth.[35,36] The time before the critical nucleus of a zeolite is formed is still too long even for this ultrafast type of dynamical simulation.

It is clear that the simulation methods have made significant progress in recent years. At the early stages of Si polymerization, fully quantum mechanical MD studies are within reach using Born–Oppenheimer[37] or Car–Parrinello[37,38] simulations. Thanks to newly developed potentials and coarse grained systems, simulations now approach the system sizes that are needed to describe the template directed zeolite synthesis in solution.

Nonetheless, each stage in the zeolite synthesis involves significant reaction barriers. This makes the chance of observing important reactive events at experimental conditions within the duration of the simulation period highly unlikely. The reaction itself is usually very fast and could fit perfectly within the window of timescales that are attainable by the simulation method. However, the system will likely spend extensively long periods within the well of the reactant state without any reactive event taking place. It is, therefore, important to have a method that focuses the costly simulation time on the important but rare reactive events, while limiting the superfluous exploration of the reactant well. In this article, we review such a method, the transition interface sampling (TIS) method,[39–41] that allows one to concentrate only on those trajectories that are important for the chemical process. Moreover, the TIS technique can calculate the frequency of occurrence of these successful trajectories within an infinitely long straightforward simulation. Hence, TIS allows the determination of the rate of the rare event.

The aim of this article is not to give a fully detailed theoretical derivation of the method. This has already been published elsewhere.[39–41] The goal of this article is to give an educative overview of the practical algorithms and their possible applications related to zeolite studies rather than on mathematical aspects.

II. Transition interface sampling

A. Historic perspectives of rare event simulations

The first theories for treating rare events from a microscopic perspective were pioneered by Eyring,[42] Wigner,[43] and Horiutu[44] about 20 years before the first MD simulation was performed.[45] They introduced the concept of transition state (TS) and the so-called TS theory (TST) approximation. Later Keck demonstrated how the TST approximation can be made exact by a dynamical correction, the transmission coefficient.[46] The actual application of these theories for molecular simulation was directed by the works of Bennett[47] and Chandler,[48] which have made this a standard approach in molecular simulation. A crucial point in this reactive flux (RF) method is the definition of a suitable reaction coordinate (RC). As a first step, the free energy needs to be determined along this RC using importance sampling techniques such as umbrella sampling (US)[49] or thermodynamic integration (TI).[50] This result alone is sufficient to obtain the TST approximation of the rate, which is an upper limit for the actual rate. In the second step, the correction to this approximation can be calculated by releasing dynamical trajectories from the top of the free energy barrier. The exact reaction rate can be calculated only when both steps are completed. Both the free energy barrier and the transmission coefficient depend on which RC is taken, but the final result that combines the two outcomes is independent of this choice.

The RF method has proved its value for many systems, but also has its drawbacks. Although its result is independent of the chosen RC, its efficiency does sensitively determine its success or failure. A non-suitable choice of RC can result in hysteresis effects in the free energy calculation, which frustrates an accurate estimation of the barrier. Besides, even if an accurate value for the free energy barrier can be obtained, the corresponding transmission coefficient will be very small and its evaluation will require an extremely large number of pathways. In practice, it has been discovered that finding a good RC can be extremely difficult in high dimensional complex systems. Notable examples are chemical reactions in solution, where the reaction mechanism often depends on highly non-trivial solvent rearrangements. Also, computer simulations of nucleation processes use very complicated order parameters to distinguish between particles belonging to the liquid and solid phase. This makes it unfeasible to construct a single RC that accurately describes the exact place of cross-over transitions. As a result, hysteresis effects and low transmission coefficients are almost unavoidable.

The problem of finding suitable RCs has driven the development of alternative methods. In 1998, Dellago *et al*. came up with an alternative method that they called transition path sampling (TPS).[51–54] This approach can be described as a MC sampling of MD pathways. Using a detailed balance technique, a set of trajectories can be collected that satisfy some predetermined criteria. For instance, one can constrain the start- and end-point of the path in such a way that each trajectory connects the reactant and product state. An important point is that this sampling of successful reactive events does not require a RC which captures the reactive mechanism, but only needs an order parameter that can distinguish between reactant and product state. In addition to this, the first series of TPS papers[51–54] also provided a route to calculate reaction rates. However, this approach has seldom been used due to its high computational cost. TPS has been claimed not to require a RC. Instead the concept of an order parameter is applied. However, the rate constant algorithm treats this order parameter in just the same way RCs are treated in other methods. Therefore, we do not make this distinction.

Luckily, the algorithmic procedure used to calculate reaction rates using the same path sampling framework improved considerably when the TIS technique was devised.[39] TIS uses a flexible path length which reduces the number of required MD steps significantly. Moreover, the TIS method also eliminates the need for so-called MC *shifting* moves that required a considerable percentage of the simulation time in the TPS scheme. In addition, one can show that the new mathematical formulation of the reaction rate is less sensitive to recrossing events which guarantees a faster convergence.

While TPS imposes the condition on the start- and end point of the path to be within certain intervals of the RC, TIS imposes an interface crossing condition. Except for the technique proposed in ref. 41, TIS needs a RC just like the original TPS scheme. The RC is required to define a set of interfaces between the stable reactant and product states. However, unlike the standard RF methods, the TIS efficiency is relatively insensitive to the choice of RC as was first proven in ref. 55. This point is a strong advantage in complex systems where a 'good RC' can be extremely difficult to find.

B. The TIS algorithm

The TIS algorithm works as follows. The first step is to define a RC and a set of related values $\lambda_0, \lambda_1, \ldots, \lambda_n$ with $\lambda_i < \lambda_{i+1}$. The subsets of phase- or configuration points for which the RC is exactly equal to λ_i basically define multidimensional surfaces or interfaces which give this method its name. These values/interfaces should obey the following requirements: if the RC is lower than $\lambda_0 = \lambda_A$, the system should be in the reactant state A; if the RC is higher than $\lambda_n = \lambda_B$ the system should be in the product state B; n and the positions for the interfaces in between, λ_i with $1 = 1, 2, \ldots, n-1$, should be set to optimize the efficiency. Further, the surface λ_A should be set in such a way that whenever a MD simulation is released from within the reactant well, this surface should be frequently crossed. The TIS rate expression can then be formulated as

$$k_{AB} = f_A \mathscr{P}_A(\lambda_B|\lambda_A) \quad (1)$$

Here, f_A is the escape flux through the first interface. In a long MD simulation, this simply corresponds to the number of detected crossings through the surface λ_A divided by the total simulation time (here, we assume that we will not observe a spontaneous transition to state B during the simulation. For a more formal definition see ref. 39). The other term $\mathscr{P}_A(\lambda_B|\lambda_A)$ is the overall crossing probability. This is the probability that whenever the system crosses λ_A, it will cross λ_B *before* it crosses λ_A again. As λ_B is a surface at the other side of the barrier, this probability will be very small and can not be calculated directly. This probability can, however, be determined by a

series of path sampling simulations using the following factorization:

$$\mathscr{P}_A(\lambda_B|\lambda_A) = \mathscr{P}_A(\lambda_n|\lambda_0) = \prod_{i=0}^{n-1} \mathscr{P}_A(\lambda_{i+1}|\lambda_i). \quad (2)$$

The terms $\mathscr{P}_A(\lambda_{i+1}|\lambda_i)$ are history dependent conditional crossing probabilities which are much higher and can be computed. In other words, $\mathscr{P}_A(\lambda_{i+1}|\lambda_i)$ is the probability that λ_{i+1} will be crossed before λ_A under the twofold condition that the system is at the point to cross the interface λ_i in one time step while λ_A was more recently crossed than λ_i in the past. It is due to this history dependence that eqn (2) is exact and should not be misinterpreted as a Markovian approximation. $\mathscr{P}_A(\lambda_{i+1}|\lambda_i)$ is also equal to the number of all possible paths that start at λ_A and end at λ_{i+1} divided by the number of all possible paths that start at λ_A, end at either λ_{i+1} or λ_A, and have at least one crossing with λ_i. Hence, this term can be calculated if we can generate the appropriate trajectories with their correct statistical weight. However generating these pathways is not obvious, especially when λ_i is in the reaction barrier region. This difficulty can be overcome by a MC algorithm that employs a variation of the TPS *shooting* move. The algorithm is explained in Fig. 1.

The algorithm requires one path to fulfil the correct condition, that is, starting at λ_A and crossing λ_i at least once before ending at either λ_{i+1} or λ_A. A crucial point is step II. After picking a random time slice (a point that constitutes all the particle positions and momenta at a certain time step along the path), one adds random values to all the momenta. In practice, these random values are taken from a Gaussian distribution with a certain width σ, that should be adapted to obtain the optimum efficiency. If σ is small, the random momentum changes will be small as well and the new path will lie close to the old one (if we assume deterministic dynamics). This small deviation results in a significant chance that the trial path will satisfy the required conditions as well which yields a good acceptance rate. However, a too small value of σ will result in too strong correlations between the accepted moves (in the extreme case when $\sigma = 0$, one regenerates exclusively the same path). Usually, one tries several values for σ in a series of short test simulations. It is generally assumed that the value which yields an acceptance rate of 50% is close to an optimum value for σ. If one wants to simulate at constant energy instead of constant temperature, step III can be replaced by a proper velocity rescaling procedure that, if needed, can also preserve linear and angular momentum.[56]

Another important point is that, in order to enter the loop, one needs to have a single path that obeys the correct requirements. This can already be quite difficult and several techniques to get such a first initial path have been suggested.[57] However, in TIS these initial paths are generated automatically when the different types of simulations are performed consecutively (see Fig. 2). First, the MD simulation is performed to calculate f_A. Then, a series of path-sampling simulations follows to calculate $\mathscr{P}_A(\lambda_1|\lambda_0)$, $\mathscr{P}_A(\lambda_2|\lambda_1)$,..., $\mathscr{P}_A(\lambda_n|\lambda_{n-1})$. When these simulations are performed in this order, each path-sampling simulation can obtain the necessary initial path from the previous simulation (see Fig. 2).

It is important to note that the final result, the reaction rate k_{AB}, does not sensitively depend on the positions of the outer interfaces λ_A and λ_B as long as they are reasonable. The number of interfaces n and their positions only influence the efficiency of the method. It was found that the total efficiency is optimized when for each path-simulation one out of five trajectories reaches the next interface.[41,55] Hence, using some initial trial simulations, one can adjust the number of interfaces and their positions to satisfy this condition. The easiest way to achieve this is to use a slight variation of the algorithm that is shown in Fig. 1. Instead of stopping the integration when the trajectory crosses λ_{i+1} as in panel (e) and (k), one can continue the trajectory until it reaches λ_A or λ_B. This algorithm only requires knowing the position of λ_A, λ_B, and λ_i. By examining the progress of the paths along the RC beyond λ_i, one can define the next interface λ_{i+1} exactly at the point where 80% of the paths have returned to λ_A.

C. Analysis of the reaction mechanism

When the complete series of simulations is finished, the reaction rate follows simply from eqn (1) and (2). In addition to this, the ensemble of pathways can be analyzed which can yield valuable information about the reaction mechanism. In this respect, the TIS path ensembles might actually prove to be more useful than the ones obtained by the original TPS method. As each ensemble contains the correct ratio of paths progressing up to a certain level, but then either return or make a little step further, one can try to understand the characteristic differences between the 'successful' and 'unsuccessful' pathways. In contrast, the TPS method aims to generate successful trajectories only. One of the properties that can improve the understanding of the mechanisms is the overall crossing probability function. This represents a sort of path survival probability along the RC. This function equals 1 at λ_0 and $P_A(\lambda_B|\lambda_A)$ at λ_B. In transition, this function is monotonically decreasing and terminates in a horizontal plateau when the barrier ridge is crossed completely. This function could be considered as a dynamical equivalent of the free energy profile along the RC. In Fig. 3 the overall crossing probability function is depicted together with the free energy profile obtained from a nucleation process of Lennard-Jones particles. The results were obtained from ref. 58. Interestingly, after the maximum free energy barrier is crossed (cluster size 243), the majority of the trajectories ($\sim$75%) still fail to reach the reactant state. This effect might be partly due to diffusive motion, but is most likely an effect of an improperly chosen RC. This shows that the projection on a single RC using static free energy calculations can be misleading. Neither the height of the barrier nor the position of the TS dividing surface have to reflect the actual height and position of the reaction barrier. Indeed, Moroni *et al.* found that a 'good RC' should at least incorporate one more important quantity which is the crystallinity of the cluster.[58] Small clusters $<$243 with a high crystallinity were found to grow larger easily, while large clusters with less structure were unstable and broke up into smaller pieces.

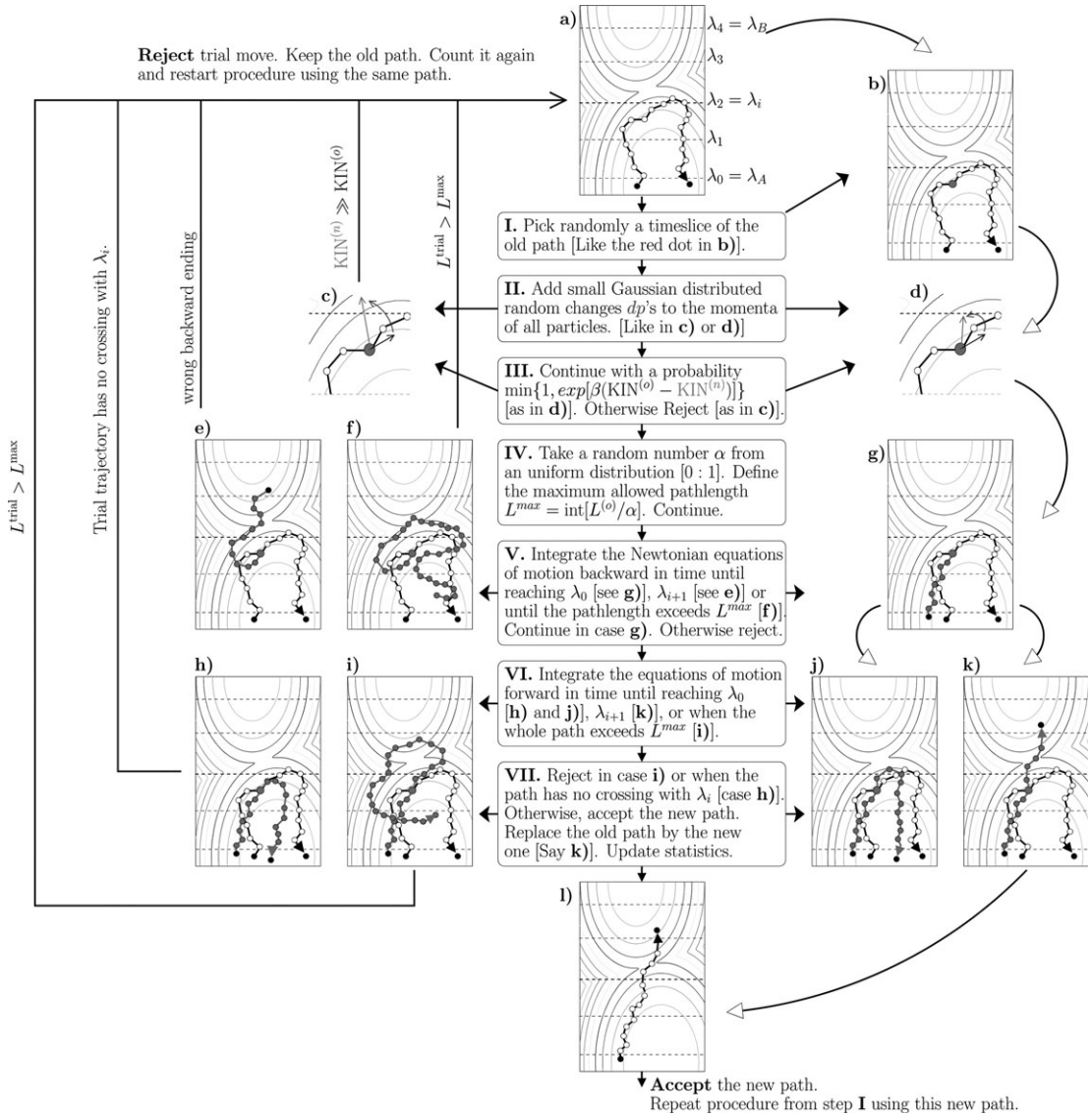

Fig. 1 Illustration of the shooting algorithm in TIS. The panels (a–l) depict trajectories/trajectory-segments on a free energy surface. The dashed horizontal lines are the TIS interfaces ($n = 4$ and $i = 2$ in this case). The algorithm requires an initial path (a) to start the loop. The length of this particular path $L^{(o)}$ is eighteen time slices (end points are not included). At step I, a random point is picked from this old path and some small randomized changes are applied to the velocities of all the particles (II), followed by a Metropolis acceptance/rejection step (III). In (c) the new velocities have resulted in a much larger kinetic energy $\text{KIN}^{(n)}$ and therefore this trial move is most likely rejected. Step IV is required to maintain detailed balance between pathways of different lengths. For example, if the random number generator assigns $\alpha = 0.59$ then $L^{\max} = 30$ and we can reject when the path is unfinished, but already contains 31 time slices as in panel (f) and (i). At (V), the equations of motion are integrated backwards in time by a MD algorithm using the shooting point with reverse velocities as starting point. At (VI) the equations of motion are integrated forward in time starting from the same shooting point (without reversed velocities). After a rejection the old path is kept and counted again. If accepted, the new path will automatically start at λ_A and cross λ_i. The path can end at either λ_A as in (j) or at λ_{i+1} as in (k). The fraction of sampled pathways that end at λ_{i+1} determines $\mathscr{P}_A(\lambda_{i+1}|\lambda_i)$.

D. Recent and future developments and applications

Besides providing an efficient algorithm for the calculation of reaction rates, the TIS method has provided a new mathematical framework for the description of rare events. Recent new simulation techniques have exploited this TIS theory. For example, for diffusive barrier crossings, where transition paths become very long, the partial path TIS (PPTIS) method was devised.[59] Here, using the assumption of memory loss, much shorter paths are generated after which the overall crossing probability can be reconstructed by a recursive formulation. The forward flux sampling technique[60,61] is basically the same as TIS, but the way in which pathways are generated is different. In this approach, the end points of all the pathways successfully reaching the next interface are stored and starting from each point a set of new pathways is generated in the next simulation. The main advantage is that the FFS scheme supplies a route for handling non-equilibrium systems. A disadvantage is that this only works for stochastic dynamics and will always yield much stronger correlations between the

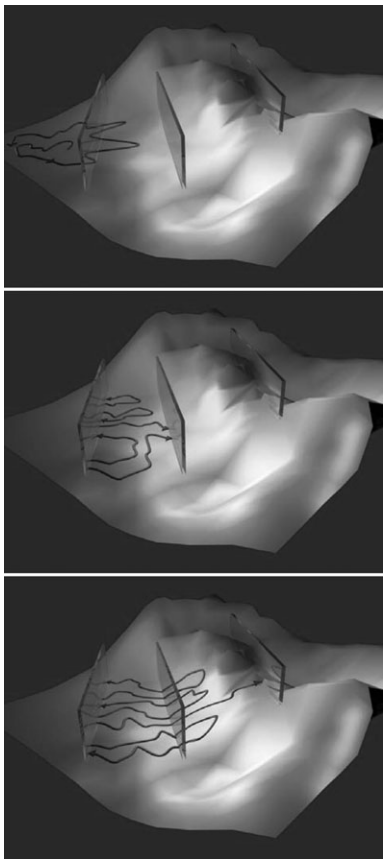

Fig. 2 This pictures illustrates some typical trajectories on a free energy surface for a series of TIS simulations. The glassy plates represent the TIS interfaces. The first type of simulation (top), is a straightforward MD simulation which is required to calculate the flux f_A through the first interface. The next step is a path-sampling simulation which generates pathways that start at λ_A and end at either λ_A or λ_1. This simulation yields the result of $\mathscr{P}_A(\lambda_1|\lambda_0)$ and is illustrated in the middle panel. The initial path to start this simulation can be obtained by taking a trajectory segment from the initial MD simulation. The bottom panel shows the next path-sampling simulation to calculate $\mathscr{P}_A(\lambda_2|\lambda_1)$. It generates pathways that start at λ_A and cross λ_1 at least once. Here, the initial path can be obtained from the previous simulation by taking one of the paths that successfully reached λ_1.

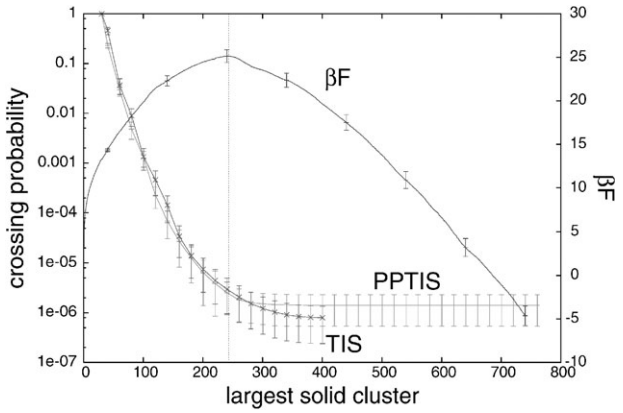

Fig. 3 The crossing probability function obtained by TIS and partial path TIS (PPTIS)[59] for the nucleation process of LJ particles. The simulation data are obtained from ref. 58. The free energy profile, which was calculated simultaneously using the technique of ref. 72, is also shown. The simulated system contained 10 648 particles in total. The RC was defined as the largest solid cluster in the system. More details can be found in ref. 58. The final crossing probability was $P_A(\lambda_B|\lambda_A) = (7.8 \pm 5.5) \times 10^{-7}$ (TIS) and $(14.1 \pm 8.7) \times 10^{-7}$ (PPTIS). The crossing probability shows a plateau at 410.5 indicating that the reaction barrier ridge is crossed. The free energy barrier has a maximum at 243. After this point about 50% (PPTIS) till 75% (TIS) of the paths still fail to reach the reactant state. Although the PPTIS and TIS results are within each others error-bars, it is likely that PPTIS overestimates the crossing probability due to the imprecise choice of RC.[55]

generated pathways and the different path ensembles, even for the pure Brownian dynamics case. Another drawback of PPTIS and FFS methods is that they do not possess the same RC insensitivity as TIS.[55] If necessary, even a fully RC free approach is possible as was suggested in ref. 41 using the TIS path length as a transition parameter. A nice feature of this approach is that it does not require one to specify a specific product state. Combinations with configurational bias MC[41,61] and path swapping techniques[41,62] may also yield promising advances for the computational efficiency.

The TIS and its variations have been applied to various systems ranging from simple test systems,[39,59] nucleation,[58,63,64] protein folding,[65,66] biochemical networks,[60] driven polymer translocation through pores,[61] micelle formation,[67] *ab initio* simulation of chemical reactions[40] and DNA denaturation.[62]

The TIS technique can open many possible avenues in the field of zeolite formation simulations at several stages of the process. For instance, the first elementary step to Si polymerization is the condensation reaction $2Si(OH)_4 \rightarrow Si_2O(OH)_6 + H_2O$. This has been studied by *ab initio* static analysis including implicit solvent.[68] This study has revealed two possible reaction mechanisms. Such a system is small enough to be treated by *ab initio* MD[37,38] including explicit solvent molecules. The TIS method could give valuable insight into which reaction mechanism dominates when dynamics and explicit solvent are taken into account. Classical reactive force fields and rare event methods, such as TIS and PPTIS, should make it possible to simulate the dynamics of Si polymerization at much lower temperatures than hitherto possible.[69] This allows the study of this process at conditions that are much closer to the experimental situation. Moreover, by the right construction of the interfaces, the TIS method allows one to focus on reaction mechanisms and rates of some very specific polymerization reactions, for instance the formation of the Si-30/33 precursor.[8]

With the development of lattice and KMC models, the study of the next stages of nucleation and zeolite growth are also within reach. The combination of KMC and path sampling is a promising yet unexplored territory. Despite the enormous long simulation periods that can be achieved by KMC, the expected length of time required to form a critical nucleus starting from a disordered solution is generally still out of reach. Therefore, most KMC studies have concentrated on growth rather than nucleation. Hence, the study of zeolite

nucleation might benefit significantly from using combined KMC and path sampling techniques.

III. Summary

We have reviewed the TIS method, its variations and possible applications for the theoretical study of zeolite synthesis. The TIS method is an elegant approach circumventing the time-scale problem, not by speeding up the dynamics of the system itself, but by concentrating on the short time trajectories which are of interest without using any approximation. TIS allows reaction barriers to be overcome by a sequence of simulation series. It is important to realize that the barrier crossing event is not enhanced due to some artificial force but is only due to the MC acception/rejection steps that include the interface crossing condition. Hence, each trajectory in the TIS path ensembles satisfies the correct dynamics on the true potential energy surface. This makes the method fundamentally different from, for instance, the metadynamics[70] approach. The TIS method makes use of the fact that the time needed to actually cross the barrier, the transition time, is much shorter than the relaxation time k_{AB}^{-1}, which is the time in which one can expect a reactive event from an arbitrary point within the reactant well.

TIS can be combined with any type of dynamics such as *ab initio* MD, Langevin, pure Brownian motion, classical MD and KMC. A requirement for the application of this method is that the simulation of short trajectories can occur sufficiently fast. This limits the size of the systems which can be studied, ranging from several molecules for *ab initio* dynamics to several thousand molecules for MD, and even larger assemblies for KMC simulations.

Still, substantial work has to be done before fully realistic modeling of zeolite synthesis is within our reach. An important requirement is the development of more accurate reactive force fields that can describe chemical events within the environment of solvent and template molecules. Recently, a more systematic approach for this development was suggested.[71] Even though the development of lattice and KMC models have made substantial steps forward, inclusion of solvent effects in lattice-type models has proven to be a difficult problem that has not yet been solved. To conclude, the simulation methods have made prodigious advancements in recent years and might ultimately give answers to important questions regarding zeolite synthesis that cannot be unambiguously accessed by experimental techniques. The TIS methods can help in obtaining dynamical information for the crucial but rare reaction steps in the zeolite process. In the near future, we are going to explore the application of TIS to the study of zeolite genesis.

Acknowledgements

This work was sponsored by the Flemish Government *via* a concerted research action (GOA), and the Belgian Government through the IAP-PAI network. T. C. acknowledges the Institute for the Promotion of Innovation through Science and Technology in Flanders (IWT-Vlaanderen) for a PhD scholarship.

References

1 B. J. Schoeman, J. Sterte and J. E. Otterstedt, *Zeolites*, 1994, **14**, 110–116.
2 J. Hedlund, B. J. Schoeman and J. Sterte, in *Progress in Zeolites and Microporous Materials*, ed. H. Chon, S.-K. Ihm and Y. S. Uh, Elsevier, Amsterdam, 1996, pp. 2203–2210.
3 R. Ravishankar, C. E. A. Kirschhock, B. J. Schoeman, P. Vanoppen, P. J. Grobet, S. Storck, W. F. Maier, J. A. Martens, F. C. De Schrijver and P. A. Jacobs, *J. Phys. Chem. B*, 1998, **102**, 2633–2639.
4 D. D. Kragten, J. M. Fedeyko, K. R. Sawant, J. D. Rimer, D. G. Vlachos, R. F. Lobo and M. Tsapatsis, *J. Phys. Chem. B*, 2003, **107**, 10006–10016.
5 J. D. Rimer, J. M. Fedeyko, D. G. Vlachos and R. L. Lobo, *Chem. Eur. J.*, 2006, **12**, 2926–2934.
6 R. Ravishankar, C. E. A. Kirschhock, P. P. Knops-Gerrits, E. J. P. Feijen, P. J. Grobet, P. Vanoppen, F. C. De Schrijver, G. Miehe, H. Fuess, B. J. Schoeman, P. A. Jacobs and J. A. Martens, *J. Phys. Chem. B*, 1999, **103**, 4960–4964.
7 S. M. Auerbach, M. H. Ford and P. A. Monson, *Curr. Opin. Colloid Interface Sci.*, 2005, **10**, 220–225.
8 C. E. A. Kirschhock, R. Ravishankar, F. Verspeurt, P. J. Grobet, P. A. Jacobs and J. A. Martens, *J. Phys. Chem. B*, 1999, **103**, 4965–4971.
9 C. E. A. Kirschhock, R. Ravishankar, L. van Looveren, P. A. Jacobs and J. A. Martens, *J. Phys. Chem. B*, 1999, **103**, 4972–4978.
10 C. T. G. Knight, J. Wang and S. D. Kinrade, *Phys. Chem. Chem. Phys.*, 2006, **8**, 3099–3103.
11 V. Nikolakis, E. Kokkoli, M. Tirrell, M. Tsapatsis and D. Vlachos, *Chem. Mater.*, 2000, **12**, 845–853.
12 W. H. Dokter, H. F. Vangarderen, T. P. M. Beelen, R. A. van Santen and W. Bras, *Angew. Chem.*, 1995, **34**, 73–75.
13 B. J. Schoeman, *Microporous Mesoporous Mater.*, 1998, **22**, 9–22.
14 C. S. Cundy and P. A. Cox, *Microporous Mesoporous Mater.*, 2005, **82**, 1–78.
15 T. M. Davis, T. O. Drews, H. Ramanan, C. He, J. S. Dong, H. Schnablegger, M. A. Katsoulakis, E. Kokkoli, A. V. McCormick, R. L. Penn and M. Tsapatsis, *Nat. Mater.*, 2006, **5**, 400–408.
16 J. C. G. Pereira, C. R. A. Catlow and G. D. Price, *J. Phys. Chem. A*, 1999, **103**, 3252–3267.
17 J. C. G. Pereira, C. R. A. Catlow and G. D. Price, *J. Phys. Chem. A*, 1999, **103**, 3268–3284.
18 M. J. Mora-Fonz, C. R. A. Catlow and D. W. Lewis, *Angew. Chem.*, 2005, **44**, 3082–3086.
19 T. T. Trinh, A. P. J. Jansen and R. A. van Santen, *J. Phys. Chem. B*, 2007, **110**, 23099–23106.
20 C. R. A. Catlow, C. M. Freeman, M. S. Islam, R. A. Jackson, M. Leslie and S. M. Tomlinson, *Philos. Mag. A*, 1988, **58**, 123–141.
21 S. Tsuneyuki, M. Tsukada, H. Aoki and Y. Matsui, *Phys. Rev. Lett.*, 1988, **61**, 869–872.
22 P. Vashishta, R. K. Kalia, J. P. Rino and I. Ebbsjo, *Phys. Rev. B*, 1990, **41**, 12197–12209.
23 B. W. H. van Beest, G. J. Kramer and R. A. van Santen, *Phys. Rev. Lett.*, 1990, **64**, 1955–1958.
24 B. P. Feuston and S. H. Garofalini, *J. Phys. Chem.*, 1990, **94**, 5351–5356.
25 C. R. A. Catlow, D. S. Coombes, D. W. Lewis and J. C. G. Pereira, *Chem. Mater.*, 1998, **10**, 3249–3269.
26 D. W. Lewis, C. R. A. Catlow and J. M. Thomson, *Faraday Discuss.*, 1997, **106**, 451–471.
27 N. Z. Rao and L. D. Gelb, *J. Phys. Chem. B*, 2004, **108**, 12418–12428.
28 M. G. Wu and M. W. Deem, *J. Chem. Phys.*, 2002, **116**, 2125–2137.
29 M. Jorge, S. M. Auerbach and P. A. Monson, *J. Am. Chem. Soc.*, 2005, **127**, 14388–14400.
30 F. R. Siperstein and K. E. Gubbins, *Stud. Surf. Sci. Catal.*, 2002, **144**, 647–654.
31 D. T. Gillespie, *J. Comput. Phys.*, 1978, **28**, 395–407.
32 M. W. Anderson, J. R. Agger, N. Hanif, O. Terasaki and T. Ohsuna, *Solid State Sci.*, 2001, **3**, 809–819.
33 M. W. Anderson, J. R. Agger, N. Hanif and O. Terasaki, *Microporous Mesoporous Mater.*, 2001, **48**, 1–9.
34 J. R. Agger, N. Hanif and M. W. Anderson, *Angew. Chem.*, 2001, **40**, 4065–4067.

35 S. Piana and J. D. Gale, *J. Am. Chem. Soc.*, 2005, **127**, 1975–1982.
36 S. Piana, M. Reyhani and J. D. Gale, *Nature*, 2005, **438**, 70–73.
37 D. Marx and J. Hütter, *Ab initio* molecular dynamics: theory and implementation, in *Modern Methods and Algorithms of Quantum Chemistry*, ed. J. Grotendorst, NIC, FZ Jülich, 2000, pp. 301–449.
38 R. Carr and M. Parrinello, *Phys. Rev. Lett.*, 1985, **55**, 2471–2474.
39 T. S. van Erp, D. Moroni and P. G. Bolhuis, *J. Chem. Phys.*, 2003, **118**, 7762–7774.
40 T. S. van Erp, *Solvent effects on chemistry with alcohols*, PhD thesis, Universiteit van Amsterdam, 2003.
41 T. S. van Erp and P. G. Bolhuis, *J. Comput. Phys.*, 2005, **205**, 157–181.
42 H. Eyring, *J. Chem. Phys.*, 1935, **3**, 107–115.
43 E. Wigner, *Trans. Faraday Soc.*, 1938, **34**, 29–41.
44 J. Horiuti, *Bull. Chem. Soc. Jpn.*, 1938, **13**, 210–216.
45 B. J. Alder and T. E. Wainwright, *J. Chem. Phys.*, 1957, **27**, 1208–1211.
46 J. C. Keck, *Adv. Chem. Phys.*, 1967, **13**, 85–121.
47 C. H. Bennett, in *Algorithms for Chemical Computations*, ACS Symposium Series No. 46, ed. R. Christofferson, American Chemical Society, Washington, DC, 1977.
48 D. Chandler, *J. Chem. Phys.*, 1978, **68**, 2959–2970.
49 G. M. Torrie and J. P. Valleau, *Chem. Phys. Lett.*, 1974, **28**, 578–581.
50 E. A. Carter, G. Ciccotti, J. T. Hynes and R. Kapral, *Chem. Phys. Lett.*, 1989, **156**, 472–477.
51 C. Dellago, P. G. Bolhuis, F. S. Csajka and D. Chandler, *J. Chem. Phys.*, 1998, **108**, 1964–1977.
52 C. Dellago, P. G. Bolhuis and D. Chandler, *J. Chem. Phys.*, 1998, **108**, 9236–9245.
53 P. G. Bolhuis, C. Dellago and D. Chandler, *Faraday Discuss.*, 1998, **110**, 421–436.
54 C. Dellago, P. G. Bolhuis and D. Chandler, *J. Chem. Phys.*, 1999, **110**, 6617–6625.
55 T. S. van Erp, *J. Chem. Phys.*, 2006, **125**, 174106.
56 P. L. Geissler, C. Dellago and D. Chandler, *Phys. Chem. Chem. Phys.*, 1999, **1**, 1317–1322.
57 P. G. Bolhuis, D. Chandler, C. Dellago and P. L. Geissler, *Annu. Rev. Phys. Chem.*, 2002, **53**, 291–318.
58 D. Moroni, P. R. ten Wolde and P. G. Bolhuis, *Phys. Rev. Lett.*, 2005, **94**, 235703.
59 D. Moroni, P. G. Bolhuis and T. S. van Erp, *J. Chem. Phys.*, 2004, **120**, 4055–4065.
60 R. J. Allen, P. B. Warren and P. R. ten Wolde, *Phys. Rev. Lett.*, 2005, **94**, 018104.
61 R. J. Allen, D. Frenkel and P. R. ten Wolde, *J. Chem. Phys.*, 2006, **124**, 024102.
62 T. S. van Erp, in preparation.
63 C. Valeriani, E. Sanz and D. Frenkel, *J. Chem. Phys.*, 2005, **122**, 194501.
64 A. J. Page and R. P. Sear, *Phys. Rev. Lett.*, 2006, **97**, 065701.
65 P. G. Bolhuis, *Proc. Natl. Acad. Sci. U. S. A.*, 2003, **100**, 12129–12134.
66 P. G. Bolhuis, *Biophys. J.*, 2005, **88**, 50–61.
67 R. Pool, *Coarse grained soap. A molecular simulation study on micelle formation in dilute surfactant solutions*, PhD thesis, Universiteit van Amsterdam, 2006.
68 J. C. G. Pereira, C. R. A. Catlow and G. D. Price, *Chem. Commun.*, 1998, **13**, 1387–1388.
69 N. Z. Rao and L. D. Gelb, *J. Phys. Chem. B*, 2004, **108**, 12418–12428.
70 A. Laio and M. Parrinello, *Proc. Natl. Acad. Sci. U. S. A.*, 2002, **99**, 12562–12566.
71 T. Verstraelen, D. van Neck, P. W. Ayers, V. van Speybroeck and M. Waroquier, *J. Chem. Theory Comput.*, submitted.
72 D. Moroni, T. S. van Erp and P. G. Bolhuis, *Phys. Rev. E*, 2005, **71**, 056709.